Acta Cryst. (1984). B40, 257–262

New Series of Superstructures Based on a Clinopyroxene. III. Higher-Order Superstructures

By Yoshio Takéuchi and Tsutomu Takahata

Mineralogical Institute, Faculty of Science, University of Tokyo, Hongo, Tokyo 113, *Japan*

and Jun Ito†

James Frank Institute, University of Chicago, Chicago, IL 60637, *USA*

(*Received* 6 *December* 1983; *accepted* 17 *February* 1984)

Abstract

The crystal structure of an En-IV-N type may be represented by a symbol (N,N), where N (=**10**, **9**, or **8**) denotes its pyroxene slab and corresponds to the number of the silicate tetrahedra that defines the slab width. The symbol means that the repeat unit consists of two N's of the same figure. The En-IV-N (and EnIV'-N) structures may further be modulated to yield a group of higher-order superstructures whose repeat units are composites of different kinds of N's. A simple class of these compound superstructures may be represented by ($\mathbf{N}^e * m, \mathbf{N}^o * n$), showing that the repeat units consist of an m succession of even N and n succession of odd N, where m and n are integers. A systematic derivation of these structures has shown that the repeat units, if m is odd, take the form ($\mathbf{N}^e * m, \mathbf{N}^o * n, \mathbf{N}^e * m, \bar{\mathbf{N}}^o * n$), where $\bar{\mathbf{N}}^o$ is the mirror image of $\mathbf{N}^o$. The structures can be classified into four groups according to their space groups. Examples observed with high-resolution transmission electron microscopy are ($\mathbf{8}, \mathbf{9}, \mathbf{8}, \bar{\mathbf{9}}$), ($\mathbf{8} * 3, \mathbf{9}, \mathbf{8} * 3, \bar{\mathbf{9}}$), and ($\mathbf{8}, \mathbf{9} * 2, \mathbf{8}, \bar{\mathbf{9}} * 2$), the c periodicities being 94·8, 184·3, and 144·9 Å, respectively. A more complicated structure, not in the above class, has been observed having the repeat unit ($\mathbf{9} * 11, \mathbf{8} * 2, \mathbf{9} * 4, \mathbf{8}, \bar{\mathbf{9}} * 2, \mathbf{8}, \mathbf{9} * 2, \mathbf{8}, \bar{\mathbf{9}}, \mathbf{8}$); this unit, 619 Å wide, is regularly repeated over a range of about one micron. Structure formulae of these compound superstructures have been discussed.

Introduction

In parts I and II (Takéuchi, Kudoh & Ito, 1984*a*; Takéuchi, Mori, Kudoh & Ito, 1984*b*) we described the structures in the chemical series of *enstatite* IV (En-IV) and *scandium series of enstatite* IV (EnIV'), each structure bearing a superstructure relation to a clinopyroxene. Three structure types which have so far been found to date in these series have been denoted En-IV-10, En-IV-9 and En-IV-8, their general form being En-IV-N. They are built up of slabs of a clinopyroxene (CPX) structure type in which the metasilicate chains have finite extensions 10, 9, or 8 tetrahedra long, respectively. The structural formula for En-IV-N expressed in an idealized form is given by

$$[Mg_{(x-12)/3}Sc_4][Li_{4/3}Si_{(x-4)/3}]O_x,$$

where $x = 124$, 112, and 100 for En-IV-10, En-IV-9, and En-IV-8, respectively. The Li atom is at a site which is denoted T and tetrahedrally coordinated. This tetrahedron is located at the boundaries of the CPX slabs and plays the role of joining together the silicate chains in adjacent slabs. In the Sc series of enstatite IV, the Li atom is missing and the T site is basically occupied by Mg, this giving an idealized formula

$$[Mg_{(x-7\cdot5)/3}Sc_3][Mg_{2/3}Si_{(x-4)/3}]O_x.$$

Both formulae imply the existence of a correlation between the structure type and the Sc/(Sc + Mg) ratio; these series of structures may thus be regarded as examples of composition-modulated superstructures.

In accordance with the difference in dimensions of the CPX slabs, their unit cells are characterized by different c lengths: 55·4, 50·0, and 44·7 Å respectively for the En-IV-10, En-IV-9, and En-IV-8 structure types. Other dimensions of the unit cells are nearly the same: $a \simeq 9{\cdot}4$, $b \simeq 8{\cdot}7$ Å, and $\beta \simeq 103°$. If N is even the space group is $B2/a$ and if odd $A2/a$. Each unit cell contains two formula units. Note that in the alternative choice of axes we use here the A set of axes (Takéuchi *et al.*, 1984*a*) in which the c axis is taken along the extension of the silicate chains of the CPX slabs.

By means of high-resolution transmission electron microscopy (HRTEM), a regular repetition was demonstrated by Takéuchi (1978) for the CPX slabs, 27 Å ($=\frac{1}{2} \times 55{\cdot}4$ Å $\times \cos \beta$) wide, of an En-IV-10 crystal. Later, however, a case was observed in which the repeat unit was a composite of two different kinds of slabs (Ozawa, Takéuchi & Mori, 1979): one is a slab of En-IV-10 type and the other of En-IV-9 type. Further HRTEM observation has shown the existence of various examples of this kind of structures which may be called *compound superstructures*. The present

† Deceased 6th June 1978.

0108-7681/84/030257-06$01.50

paper describes those higher-order superstructures characteristic of the chemical series now considered. As geometrical principles of combining different kinds of slabs are the basis for describing the compound superstructures, they are given first.

Derivation of the compound superstructures

Symbolism of the basic superstructures

We now adopt the symbol **N** of an En-IV-*N* structure type to denote the type of its CPX slab. The unit cell of the *A* type of an En-IV-*N* structure, regardless of its structure type, contains two slabs related to each other by a twofold rotation. The periodical repetition of the unit cell to yield the structure may then be expressed by a symbol (**N**,**N**). Thus, for example, the En-IV-10 or En-IV-9 structure types are expressed by (**10**,**10**) or (**9**,**9**), respectively.

Combination of different types of slabs

The geometrical features of the CPX slab of an En-IV-*N* structure may well be represented by the portion of the slab bounded by $x=0$ and $x=\frac{1}{2}$ of the unit cell for the purpose of studying the combination of different types of slabs. That portion of slab **8** is illustrated in Fig. 1 as a representative of the family of even **N** (=$\mathbf{N}^e$). The corresponding portion of slab **9** is given in Fig. 2 as a representative of odd **N** (=$\mathbf{N}^o$). Although the silicate chains in each diagram are depicted as a stretched form, it does not spoil the essential geometrical features of the slab. Each pair of the boundaries of a slab so expressed is represented by an array of *T*'s, along **b**, on the same twofold rotation axis **δ**. When we combine two slabs, they must be juxtaposed in parallel position so that they share the *T*'s at the adjoining boundary of the slabs. Details of the links of the polyhedra that form a boundary are given in Fig. 6 of part I (Takéuchi *et al.*, 1984*a*).

A comparison of these diagrams reveals the following important differences between **8** and **9**:

(*a*) The tetrahedra *T*'s in one boundary of **8** are displaced, along **b**, by $b/4$ (or $3b/4$) relative to those in the other boundary. In slab **9**, however, *T*'s in one boundary are displaced, relative to those in the other, by $b/2$.

(*b*) *T*'s in one boundary of slab **8** are enantiomorphic to those in the other. This relation arises from the fact that the portion of the unit cell now considered has centres of symmetry as indicated in Fig. 1. On the other hand, all *T*'s in **9** are congruent (Fig. 2). Accordingly, for the present purpose of deriving the repetition units which are composites of several **8**'s and several **9**'s, we consider the enantiomorphic analogue of **9**. We hence introduce a symbol $\bar{\mathbf{9}}$ to denote such a symmetrical counterpart of **9** (Fig. 2*c*).

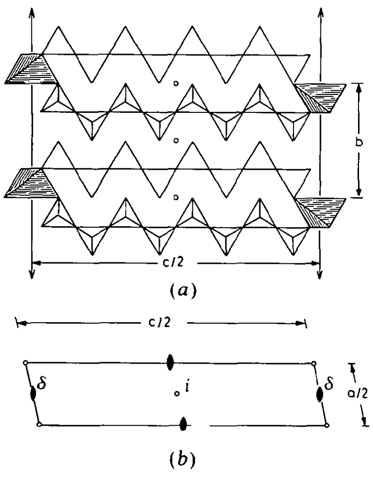

Fig. 1. (*a*) The structure of slab **8** viewed down **a*** and bounded by $x=0$ and $x=\frac{1}{2}$ showing only the silicate chains in an idealized stretched form. Twofold axes are indicated that pass through the ruled tetrahedra *T*'s, small circles indicating the centres of symmetry. The twofold axes correspond to those denoted **δ** in (*b*) which shows, down **b**, the locations of twofold axes and centres of symmetry.

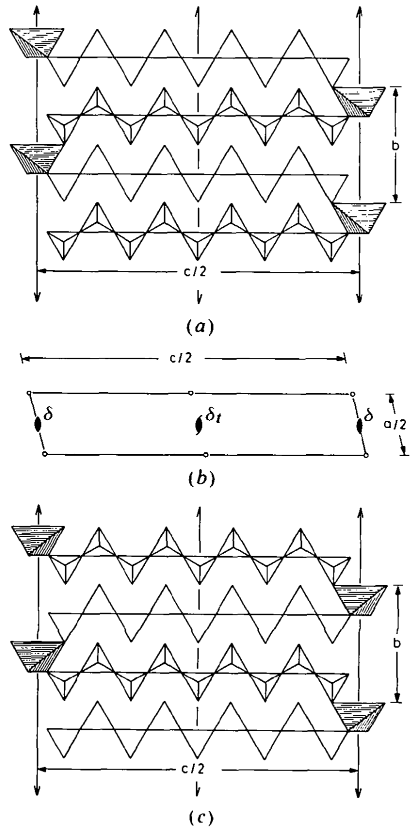

Fig. 2. (*a*) The structure of slab **9**, illustrated in a way which is similar to the case of **8** (Fig. 1*a*). A pair of twofold axes **δ** passing through *T* (ruled) and a twofold screw axis $\boldsymbol{\delta}_t$ are shown. (*b*) The locations of **δ** and $\boldsymbol{\delta}_t$ viewed down **b**. (*c*) Slab $\bar{\mathbf{9}}$ which is a mirror image of **9** shown in (*a*).

Now, consider the cases of composite superstructures in which a succession of $\mathbf{N}^e$ and another succession of $\mathbf{N}^o$ occur alternately. Then we find from the above relations the following rules for combining slabs:

(1) If the number of successive $\mathbf{N}^e$'s is even in the sequence of slab symbols that represents a repeat unit, the symbol that immediately precedes the succession of $\mathbf{N}^e$ should be the same as the one that immediately follows it. If odd, they may be preceded by $\mathbf{N}^o$ (or $\bar{\mathbf{N}}^o$) and followed by $\bar{\mathbf{N}}^o$ (or $\mathbf{N}^o$). This rule is applicable regardless of the number of successions. An example of the former case is:

$$\ldots\mathbf{9889889889}\ldots(\mathbf{9},\mathbf{8},\mathbf{8}).$$

That for the latter is:

$$\ldots\bar{\mathbf{9}}\mathbf{888988}\bar{\mathbf{8}}\bar{\mathbf{9}}\mathbf{8889}\ldots(\bar{\mathbf{9}},\mathbf{8},\mathbf{8},\mathbf{8},\mathbf{9},\mathbf{8},\mathbf{8},\mathbf{8}).$$

Let $\mathbf{N}*n$ be a symbol that represents the n succession of $\mathbf{N}$ where n is an integer larger than unity. Then, the above symbols for the compound superstructures are given by new forms: $(\mathbf{9},\mathbf{8}*2)$ and $(\bar{\mathbf{9}},\mathbf{8}*3,\mathbf{9},\mathbf{8}*3)$, respectively.

(2) A succession such as $\bar{\mathbf{N}}^o\mathbf{N}^o$ is not permissible.

(3) In a succession of symbols, both sides of $\mathbf{N}^o$ (or $\bar{\mathbf{N}}^o$) must be the same.

(4) The a glides of the slabs are retained regardless of the types of combination.

Space group

As will be observed in Fig. 1, the symmetry characteristic of $\mathbf{N}^e$ is represented by an array, along $\mathbf{c}$, of the following symmetry elements

$$\boldsymbol{\delta}\ \boldsymbol{i}\ \boldsymbol{\delta}. \qquad (1)$$

While, that of $\mathbf{N}^o$ is represented by

$$\boldsymbol{\delta}\ \boldsymbol{\delta}_t\ \boldsymbol{\delta}. \qquad (2)$$

Then the array of symmetry elements corresponding to a succession $\mathbf{N}^e\mathbf{N}^o$ is given by

$$\boldsymbol{\delta}\ \boldsymbol{i}\ \boldsymbol{\delta}\ \boldsymbol{\delta}_t\ \boldsymbol{\delta}.$$

Thus, for example, the corresponding array of symmetry elements for the periodic structure $(\mathbf{8},\mathbf{9},\mathbf{8},\bar{\mathbf{9}})$ is

$$\ldots\boldsymbol{\delta}\ \boldsymbol{i}\ \boldsymbol{\delta}\ \boldsymbol{\delta}_t\ \boldsymbol{\delta}\ \boldsymbol{i}\ \boldsymbol{\delta}\ \boldsymbol{\delta}_t\ \boldsymbol{\delta}\ \boldsymbol{i}\ \boldsymbol{\delta}\ \boldsymbol{\delta}_t\ \boldsymbol{\delta}\ldots$$

Since the twofold axes $\boldsymbol{\delta}$ at the slab boundaries are obviously suppressed in this particular case, the symmetry elements retained in the above array are

$$\ldots\boldsymbol{i}\ \boldsymbol{\delta}_t\ \boldsymbol{i}\ \boldsymbol{\delta}_t\ \boldsymbol{i}\ \boldsymbol{\delta}_t\ldots \qquad (3)$$

Noting that the compound superstructures now considered are monoclinic and have a glides, and that the twofold axes other than $\boldsymbol{\delta}$ in $\mathbf{8}$ and some inversion centers other than $\boldsymbol{i}$'s are retained, we can readily find that the array of symmetry elements (3) which is parallel to $\mathbf{c}$ is that characteristic of $I2/a$. The space group of the above periodic structure (superstructure) is thus determined. The cell dimensions of the structure are $a=9{\cdot}4$, $b=8{\cdot}7$, $c=94{\cdot}8$ Å, and $\beta=103°$. In any case, the essential key to derive the space group can be provided by studying, as demonstrated above, the combination of (1) and (2) corresponding to the slab sequence. As a result, the compound superstructures have been found to have one of the four space groups as listed in Table 1 depending upon whether the number of the succession of $\mathbf{N}^e$ (or $\mathbf{N}^o$) is even or odd. From this result, we find that the space group for $(\mathbf{9},\mathbf{10}*2)$ is not $P2/a$ as reported previously (Ozawa *et al.*, 1979) but $A2/a$.

The space group of any other compound superstructures, not in the above category, may be readily derived in a way which is similar to the above case.

Table 1. *Classification of the compound superstructures of the* $(\mathbf{N}^e*m, \mathbf{N}^o*n)$ *type, and unit slabs of the basic structures*

Compound superstructures

m	n	Space group	Example Symbol	$d_{(001)}$
Odd	Odd	C_{2h}^6 $I2/a$	$(\mathbf{8}*3, \mathbf{9}, \mathbf{8}*3, \bar{\mathbf{9}})$	179·6 Å
Even	Odd	C_{2h}^6 $A2/a$	$(\mathbf{8}*2, \mathbf{9}*3)$†	116·8 × 2
Odd	Even	C_{2h}^4 $B2/a$	$(\mathbf{8}, \mathbf{9}*2, \mathbf{8}, \bar{\mathbf{9}}*2)$	141·2
Even	Even	C_{2h}^4 $P2/a$	$(\mathbf{10}*4, \mathbf{9}*2)$†	156·8

Basic superstructures

Structure type	Space group	$d_{(001)}$	Unit slab Symbol	Width
En-IV-10	C_{2h}^4 $B2/a$	54·0 Å	**10**	27·0 Å
En-IV-9	C_{2h}^6 $A2/a$	48·8	**9**	24·4
En-IV-8	C_{2h}^4 $B2/a$	43·6	**8**	21·8

† Hypothetical.

HRTEM observation

Specimens

Samples obtained from eight different runs of crystal synthesis were subjected to HRTEM observation. Five belonged to the En-IV series and three to the EnIV′. Their chemical compositions were studied with an electron microprobe, and structure types by the X-ray precession method. Crystals of each sample were crushed in an agate mortar to yield fragments of about several microns in size and then dispersed on carbon-coated microgrids. The HRTEM specimens thus prepared were examined with a JEOL 100-CX transmission electron microscope equipped with a goniometer stage. The specimens were tilted so that a selected zone axis became parallel to the incident beam. Direct magnification was about $6{\cdot}7\times10^4\sim1{\cdot}0\times10^5$.

By means of electron diffraction patterns, a search was made for the fragments which exhibited composite diffraction patterns, such as that given in Fig.

3 of part II (Takéuchi *et al.*, 1984*b*), or diffuse streaks. As a result, the fragments from one of the EnIV′ samples, in particular, were found to show several types of well defined compound superstructures. This specific sample was that from which we obtained a crystal piece to determine the EnIV′-9 structure type (see part II). The electron diffraction patterns did show that the crystal fragments were dominantly of the EnIV′-9 type although they tended to be composite with the EnIV′-8 type. As the chemical composition of the crystal piece used for structure determination is close to the ideal chemical formula for EnIV′-9 (part II), we may adopt the following ideal formula of EnIV′-9 for subsequent discussion:

$$[\mathrm{Mg}_{34\cdot83}\mathrm{Sc}_3\square_{1/6}]_{\Sigma=38}[\mathrm{Mg}_{2/3}\square_{4/3}\mathrm{Si}_{36}]_{\Sigma=38}\mathrm{O}_{112}. \qquad (4)$$

Results

In conformity with the fact that the crystal specimens used were frequently composite mainly of the EnIV′-9 and EnIV′-8 types, the compound superstructures observed consisted of slabs **8** and **9**. The lattice fringe images of three of them are given in Fig. 3. As the extension of some of the lattice fringe images regularly extends well over one micron, the corresponding composite structures are described below.

One, which is shown in Fig. 3(*a*), consists of an alternating sequence of **8** and **9**. The periodic unit is then given by $(\mathbf{8}, \mathbf{9}, \mathbf{8}, \bar{\mathbf{9}})$. If we assume for slab **8** the following ideal chemical composition (part II)

$$[\mathrm{Mg}_{30\cdot83}\mathrm{Sc}_3\square_{1/6}]_{\Sigma=34}[\mathrm{Mg}_{2/3}\square_{4/3}\mathrm{Si}_{32}]_{\Sigma=34}\mathrm{O}_{100}, \qquad (5)$$

we can readily calculate, in terms of (4) and (5), the possible chemical composition for this compound superstructure. The chemical formula thus derived is

$$[\mathrm{Mg}_{32\cdot83}\mathrm{Sc}_3\square_{1/6}]_{\Sigma=36}[\mathrm{Mg}_{2/3}\square_{4/3}\mathrm{Si}_{34}]_{\Sigma=36}\mathrm{O}_{106}.$$

Calculated crystallographic data are: $M_r = 3599\cdot9$, $d_{(001)} = 92\cdot4$ Å, $c = 94\cdot8$ Å, $V = 7556\cdot4$ Å^3, $Z = 4$, $I2/a$.

The lattice image shown in Fig. 3(*b*) consists of an alternating sequence of $\mathbf{8}*3$ and **9**. As this is again the case in which both m and n are odd, its periodic unit is given by $(\mathbf{8}*3, \mathbf{9}, \mathbf{8}*3, \bar{\mathbf{9}})$. Calculated structural data are:

$$[\mathrm{Mg}_{31\cdot83}\mathrm{Sc}_3\square_{1/6}]_{\Sigma=35}[\mathrm{Mg}_{2/3}\square_{4/3}\mathrm{Si}_{33}]_{\Sigma=35}\mathrm{O}_{103},$$

$M_r = 3499\cdot5$, $d_{(001)} = 179\cdot6$ Å, $c = 184\cdot3$ Å, $V = 14\,685\cdot8$ Å^3, $Z = 8$, $I2/a$.

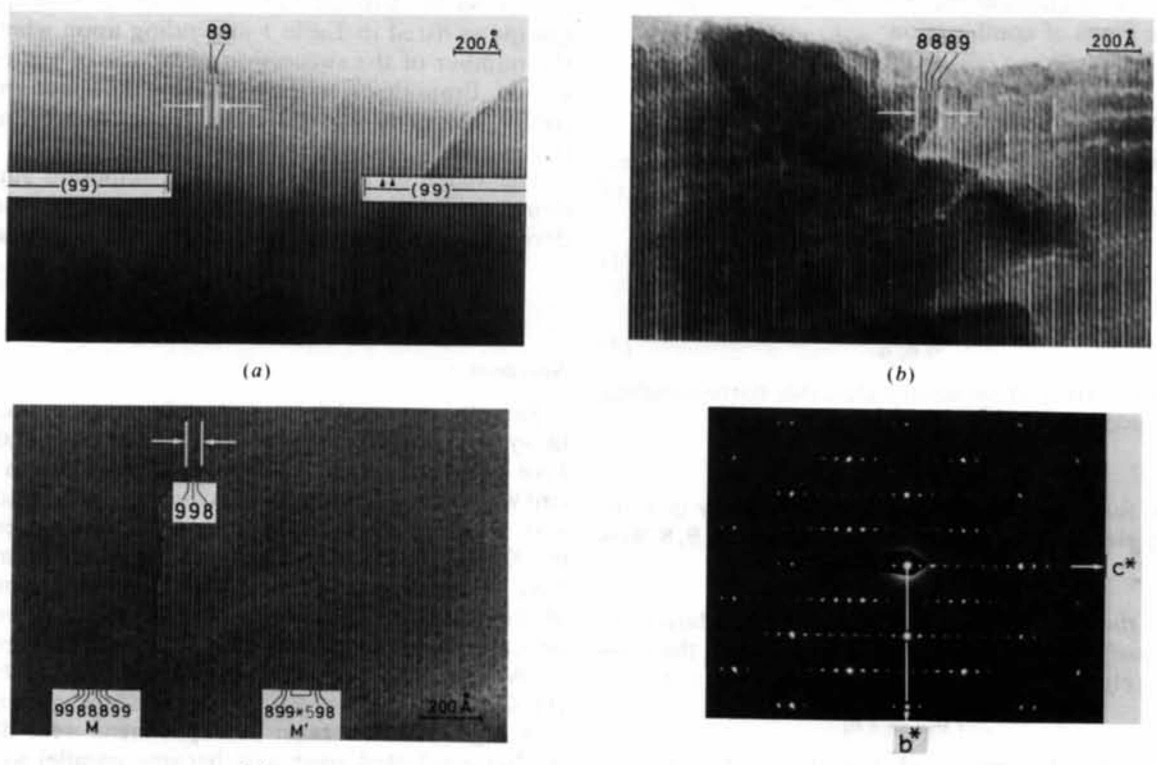

Fig. 3. Electron micrographs showing composite superstructures. (*a*) **(8, 9)** occurring in a basic structure **(9, 9)**, each triangle indicating the intergrowth of **8** in the basic structure. (*b*), **(8∗3, 9)**. (*c*) **(9∗2, 8)**. Two mistakes M and M' are indicated in the regular sequence of the repeat units, the former being characterized by the intergrowth of one excess **8**, and the latter by that of three excess **9**'s. (*d*) The electron diffraction pattern corresponding to the lattice fringe image (*b*). In each electron image, the repeat unit is indicated by a pair of white arrows.

The third image (Fig. 3*c*) is characterized by a regular alternation of $\mathbf{9} * 2$ and **8**, providing an example of the *m* odd, *n* even case (Table 1). The periodic unit is then composed of six unit slabs: ($\mathbf{9} * 2$, **8**, $\bar{\mathbf{9}} * 2$, **8**).

$[Mg_{33\cdot50}Sc_3\square_{1/6}]_{\Sigma=36\cdot66}[Mg_{2/3}\square_{4/3}Si_{34\cdot66}]_{\Sigma=36\cdot66}O_{108}$, $M_r = 3666\cdot8$, $d_{(001)} = 141\cdot2$ Å, $c = 144\cdot9$ Å, $V = 11\,547\cdot3$ Å^3, $Z = 6$, $B2/a$.

In contrast to the above examples of lattice images showing moderately complex structures, one shown in Fig. 4 is notable. A closer examination of the lattice image has revealed that the periodic unit consists of 26 slabs with the sequence ($\mathbf{9} * 11$, $\mathbf{8} * 2$, $\mathbf{9} * 4$, **8**, $\bar{\mathbf{9}} * 2$, **8**, $\mathbf{9} * 2$, **8**, $\bar{\mathbf{9}}$, **8**). This unit is regularly repeated over a range of about one micron. Calculated structural data are:

$[Mg_{33\cdot9}Sc_3\square_{1/6}]_{\Sigma=37\cdot07}[Mg_{2/3}\square_{4/3}Si_{35\cdot07}]_{\Sigma=37\cdot07}O_{109\cdot2}$, $M_r = 3707\cdot19$, $d_{(001)} = 618\cdot8$ Å, $c = 635\cdot1$ Å, $V = 50\,605\cdot5$ Å^3, $Z = 26$, Pa.

Discussion

As both the En-IV-N and EnIV′-N structures themselves are composition-modulated superstructures, we may regard that the compound superstructures, now considered, belong to the category of structures resulting from compositional higher-order modulations. The fourth example above (Fig. 4), among others, provides a remarkable feature of the higher-order modulations. In the above-mentioned symbol for this structure, the number of the succession of **9** with intervals of $\mathbf{8} * 2$ or **8** shows a stepwise decrease from left to right. The sequence of the symbols may be divided into four parts to yield the expression ($P\,Q\,R\,S$) for the repeat unit, where $P = [\mathbf{9} * 11, \mathbf{8} * 2]$, $Q = [\mathbf{9} * 4, \mathbf{8}]$, $R = [\bar{\mathbf{9}} * 2, \mathbf{8}, \mathbf{9} * 2, \mathbf{8}]$ and $S = [\bar{\mathbf{9}}, \mathbf{8}]$. The Sc/(Sc + Mg) ratios calculated for P, Q, R, and S are 0·0792, 0·0796, 0·0807, and 0·0823, respectively, thus showing a stepwise increase of the ratio in the repeat unit (these values are to be compared with 0·0779 for **9** and 0·0867 for **8**). It is remarkable that

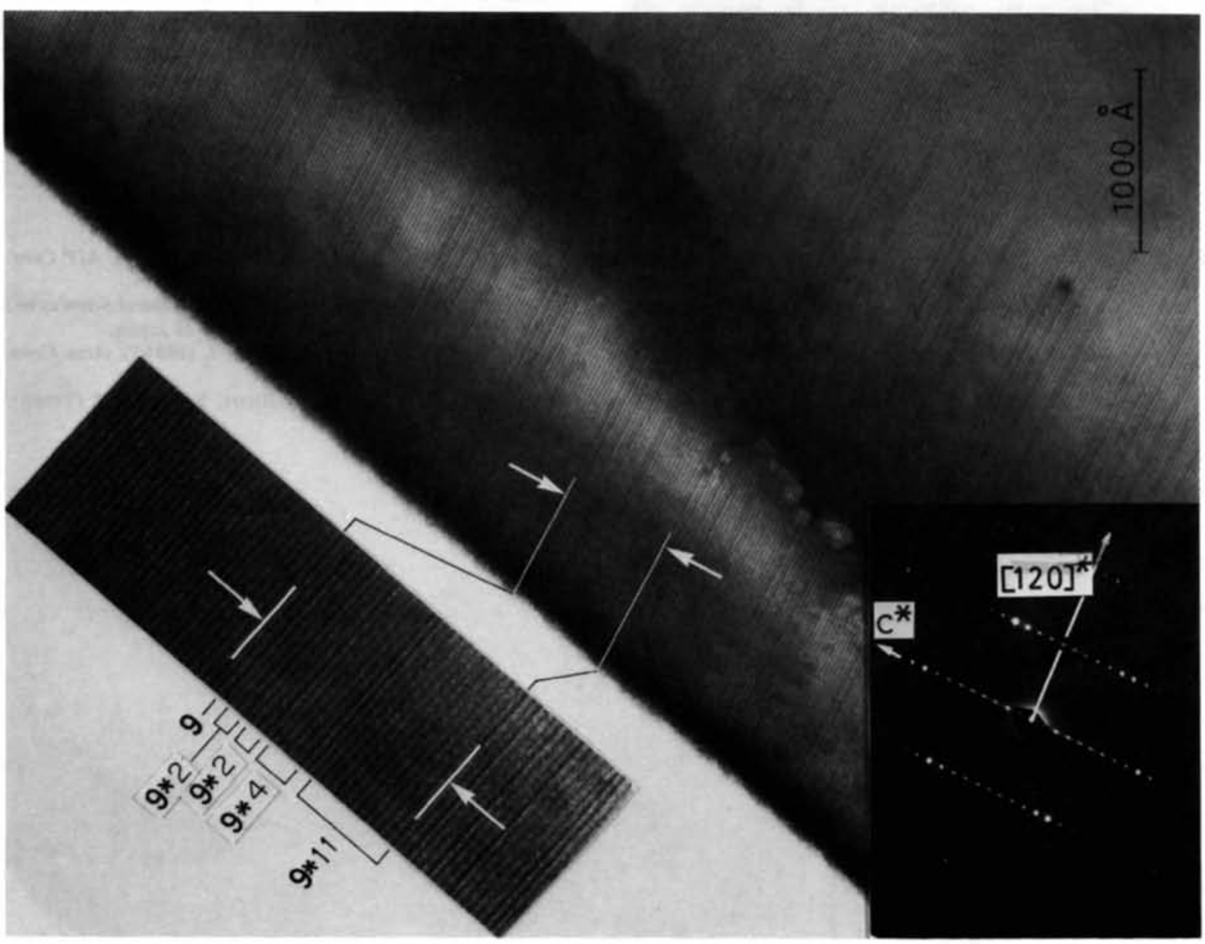

Fig. 4. Electron micrograph showing the compound superstructure ($\mathbf{9} * 11$, $\mathbf{8} * 2$, $\mathbf{9} * 4$, **8**, $\bar{\mathbf{9}} * 2$, **8**, $\mathbf{9} * 2$, **8**, $\bar{\mathbf{9}}$, **8**). The repeat unit indicated by a pair of white arrows is enlarged and shown below the unit, indicating the slab **9**'s (**9** and $\bar{\mathbf{9}}$ are not distinguished and slab **8**'s are not indicated).

such a stepwise change in minor chemical composition taking place in a linear range of about 619 Å repeats for a long range as mentioned above.

Since details of the phase diagrams for En-IV and EnIV' are not fully known (Takéuchi, 1978; Takéuchi *et al.*, 1984*a*), it is difficult to discuss the kinetics of crystal formation that yield the composite superstructures. Our observation, however, shows that they tend to occur, in a crystal fragment, between the regions having different basic-structure types. Each composite superstructure was presumably generated under a specific condition of the melt which was compositionally fluctuating from the state yielding one structure type towards that yielding another. Besides the coherent composition modulations that generate regular composite superstructures, incoherent (or irregular) modulations are also frequently observed between two different structure types. We give in Fig. 5 an example of lattice images that shows incoherent modulations taking place between basic superstructures.

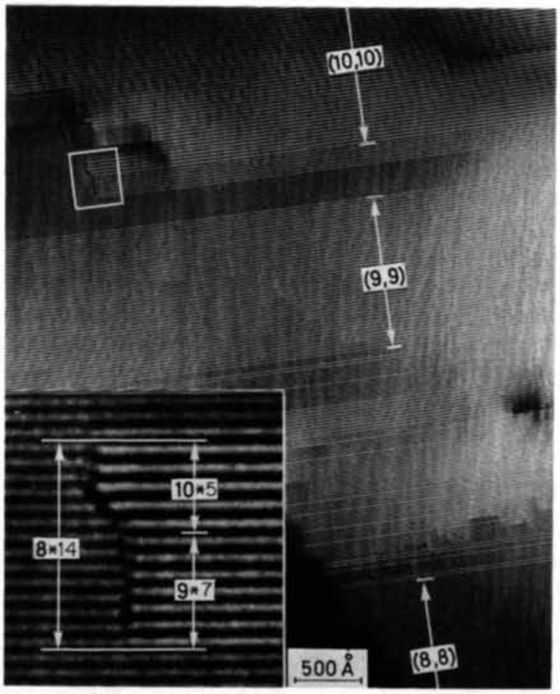

Fig. 5. Incoherent modulations taking place between the regions having different basic-structure types indicated. The area indicated by a rectangle is enlarged and given at the bottom, showing that the width of the succession **9** * 7, **10** * 5, terminating in a region of the (**8**, **8**) type, coincides with that of **8** * 14. A calculation, using the slab widths given in Table 1, yields 305·8 Å for the former and 305·2 Å for the latter, showing good agreement between the two.

Part of the crystal syntheses were carried out under the supervision of Professor O. J. Kleppa, Materials Research Laboratory of the University of Chicago, funded by the National Science Foundation; we are grateful to him for his encouragement. We wish to thank Dr Ian M. Steele for his electron microprobe analyses, and Dr A. G. L'Eprevier for his assistance with the crystal synthesis. The structural study was supported by Grant-in-Aid for Scientific Research 242016 of the Ministry of Education of Japan.

References

OZAWA, T., TAKÉUCHI, Y. & MORI, H. (1979). *AIP Conf. Proc.* No. 53, pp. 324–326.

TAKÉUCHI, Y. (1978). *Recent Progress of Natural Sciences in Japan.* Vol. 3, pp. 153–172, Science Council of Japan.

TAKÉUCHI, Y., KUDOH, Y. & ITO, J. (1984*a*). *Acta Cryst.* **B40**, 115–125.

TAKÉUCHI, Y., MORI, H., KUDOH, Y. & ITO, J. (1984*b*). *Acta Cryst.* **B40**, 126–132.